

PROGRESS IN NONEQUILIBRIUM QUANTUM FIELD THEORY *

JÜRGEN BERGES[†] AND JULIEN SERREAU[‡]

*Institut für Theoretische Physik der Universität Heidelberg
Philosophenweg 16, 69120 Heidelberg, Germany*

We review recent developments for the description of far-from-equilibrium dynamics of quantum fields and subsequent thermalization.

1. Far-from-equilibrium quantum fields

The advent of relativistic heavy-ion collision experiments as well as rapid progress in cosmological observations triggered an enormous increase of interest in the dynamics of quantum fields out of equilibrium. Much progress has been achieved for systems close to thermal equilibrium using (non-)linear response techniques or with effective descriptions based on a separation of scales in the weak coupling limit^{1,2}. These methods provide an efficient description of the dynamics on sufficiently long time scales in their range of applicability. Major open questions for our theoretical understanding are currently highlighted by experimental indications of early thermalization in collision experiments starting from extreme nonequilibrium situations^{3,4}. They provide an important motivation to study the far-from-equilibrium dynamics of quantum fields and subsequent thermalization from first principles.

There are few necessary ingredients to describe far-from-equilibrium quantum fields. Firstly, in contrast to close-to-equilibrium field theory, the initial density matrix can deviate substantially from thermal equilibrium. Fully equivalent to the specification of a density matrix is a description of the nonequilibrium initial conditions in terms of correlation functions. Secondly, nonequilibrium time evolution involves no other dynamics than the one dictated by the underlying quantum field theory. In particular, the dynamics can be conveniently obtained from the effective action Γ for given

*Prepared for SEWM2002. Based on an invited talk by J.B. and a poster by J.S.

[†]email: j.berges@thphys.uni-heidelberg.de

[‡]email: serreau@thphys.uni-heidelberg.de

initial correlation functions. Since Γ is a Legendre transform of the generating functional for connected Green’s functions, there are very efficient approximation schemes available.

Practicable and systematic approximations for nonequilibrium situations may be based on the two-particle irreducible (2PI) effective action^{5,6,7}. It has been recently demonstrated for scalar^{8,9,10} and fermionic¹¹ quantum field theories that a systematic coupling–expansion⁵ or $1/N$ –expansion^{5,9,12} of the 2PI effective action can describe far-from-equilibrium dynamics and subsequent thermalization without further assumptions. At lowest nontrivial order these approximations contain scattering contributions including off-shell and memory effects. In particular, the 2PI $1/N$ –expansion has been shown to solve the problem of an analytic description of the dynamics at nonperturbatively large densities^{13,14}.

A related approach that has been successfully applied¹⁰ to nonequilibrium quantum field theory is motivated by truncating Schwinger-Dyson equations¹⁵. It is equivalent to an approximation including the complete next-to-leading order (NLO) contribution and part of the NNLO graphs of the 2PI $1/N$ –expansion¹². Similar to the 2PI effective action technique, promising approximation schemes may also be obtained in a systematic way by considering so-called two-particle “point-irreducible” (2PPI) graphs. In the context of nonequilibrium this has been investigated in Ref. 16.

These methods provide a systematic and practical tool to go beyond standard mean-field type approximations¹⁷, such as Hartree(–Fock) or leading order large- N . Although the latter present a useful guide for various problems, they e.g. fail to describe exponential damping of correlations at early times or the late-time dynamics leading to thermalization⁸.^a These problems are related to the appearance of an infinite number of conserved quantities, which are not present in the fully interacting or finite- N field theory. The spurious constants of motion restrict the nonequilibrium evolution at all times and prevent an approach to thermal equilibrium. Although a straightforward task in principle, going beyond mean-field type approximations has long been a major difficulty in practice: Similar to perturbation theory, standard approximations based on $1/N$ –expansions of the one-particle irreducible (1PI) effective action can be secular in time. Even for small couplings these approximations break down after a short time and do not describe thermalization¹⁹. In the following we review two-particle irreducible expansion schemes and recent nonequilibrium applications.

^aFor somewhat improved results using inhomogeneous mean fields see Ref. 18.

2. 2PI effective action for scalar and fermionic fields

Consider a theory describing N scalar fields φ_a and N_f fermion flavours ψ_i with classical action ($a, b = 1 \dots N$; $i, j = 1 \dots N_f$)

$$S[\varphi; \bar{\psi}, \psi] = \int d^4x \left\{ \frac{1}{2} \partial_\mu \varphi_a \partial^\mu \varphi_a + \bar{\psi}_i(x) i \not{\partial} \psi_i(x) + V(\varphi; \bar{\psi}, \psi) \right\}. \quad (1)$$

Here $V(\varphi; \bar{\psi}, \psi)$ parametrizes the interaction part to be specified later, and $\not{\partial} \equiv \gamma_\mu \partial^\mu$ with Dirac matrices γ_μ ($\mu = 0 \dots 3$). All Green's functions of this theory can be obtained from the 2PI effective action⁵, which is parametrized by the connected one- and two-point functions:

$$\phi_a(x) \equiv \langle \varphi_a(x) \rangle, \quad G_{ab}(x, y) \equiv \langle T_c \varphi_a(x) \varphi_b(y) \rangle - \phi_a(x) \phi_b(y),$$

and similarly for the fermionic fields. Here, the field operators are time-ordered along a closed time path \mathcal{C} , as depicted in Fig. 1. For a vanishing fermionic “background” field the 2PI effective action can be written as⁵

$$\begin{aligned} \Gamma[\phi, G; D] = & S[\phi; 0, 0] + \frac{i}{2} \text{Tr}_c \ln G^{-1} + \frac{i}{2} \text{Tr}_c G_0^{-1} G \\ & - i \text{Tr}_c \ln D^{-1} - i \text{Tr}_c D_0^{-1} D + \Gamma_2[\phi, G; D], \end{aligned} \quad (3)$$

where the classical inverse propagator for the scalars is given by

$$iG_{0,ab}^{-1}(x, y; \phi) = \left. \frac{\delta^2 S[\phi; \bar{\psi}, \psi]}{\delta \phi_b(y) \delta \phi_a(x)} \right|_{\bar{\psi}=\psi=0} \quad (4)$$

and equivalently for the classical inverse fermion propagator iD_0^{-1} . The term $\Gamma_2[\phi, G; D]$ in Eq. (3) contains all contributions beyond one-loop order and can be represented as a sum over closed 2PI graphs only⁵, i.e. diagrams which cannot be disconnected by opening two propagator lines. The equations of motion are obtained by extremizing the effective action:

$$\frac{\delta \Gamma[\phi, G; D]}{\delta \phi_a(x)} = 0, \quad \frac{\delta \Gamma[\phi, G; D]}{\delta G_{ab}(x, y)} = 0, \quad \frac{\delta \Gamma[\phi, G; D]}{\delta D_{ij}(x, y)} = 0. \quad (5)$$

The resulting equations of motion can be written as differential equations suitable for initial value problems (for details see e.g. Ref. 9). All higher n -point functions can then be obtained from the generating functional $\Gamma[\phi, G; D]$ at any time during the evolution. Without further truncation the effective action contains the complete information.

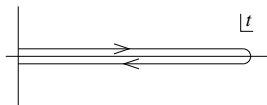


Figure 1. Traces involve a *finite* closed time path \mathcal{C} suitable for the initial value problem with a causal time evolution.

3. Systematic approximation schemes

A major advantage of the 2PI effective action is that it allows one to obtain suitable approximation schemes for nonequilibrium problems in a systematic way. As an example, we consider first a scalar field theory with $O(N)$ -symmetric classical action given by Eq. (1) with

$$V(\varphi) = \frac{m_0^2}{2} \varphi_a \varphi_a + \frac{\lambda}{4!N} (\varphi_a \varphi_a)^2. \quad (6)$$

One can classify the various contributions to the 2PI effective action according to their scaling with N . More generally, one can write the sum of 2PI diagrams as

$$\Gamma_2[\phi, G] = \Gamma_2^{\text{LO}}[\phi, G] + \Gamma_2^{\text{NLO}}[\phi, G] + \Gamma_2^{\text{NNLO}}[\phi, G] + \dots$$

where $\Gamma_2^{\text{LO}} \sim N$, $\Gamma_2^{\text{NLO}} \sim 1$, $\Gamma_2^{\text{NNLO}} \sim 1/N$ and so on, such that each following contribution is suppressed by an additional power of $1/N$. The leading order contribution corresponds to only one diagram and reads⁵

$$\Gamma_2^{\text{LO}}[G] = -\frac{\lambda}{4!N} \int_x G_{aa}(x, x) G_{bb}(x, x). \quad (8)$$

Here we use the notation $\int_x \equiv \int_c dx^0 \int dx$. The full next-to-leading contribution contains an infinite series of 2PI diagrams which can be summed:^{8,12}

$$\Gamma_2^{\text{NLO}}[\phi, G] = \frac{i}{2} \text{Tr}_c \ln[\mathbf{B}(G)] + \frac{i\lambda}{6N} \int_{xy} \mathbf{I}(x, y; G) \phi_a(x) G_{ab}(x, y) \phi_b(y), \quad (9)$$

where

$$\mathbf{B}(x, y; G) = \delta_c(x - y) + i \frac{\lambda}{6N} G_{ab}(x, y) G_{ab}(x, y),$$

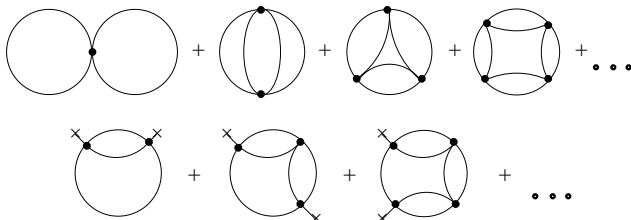


Figure 2. The complete NLO contribution to Γ_2 . The dots indicate that each diagram is obtained from the previous one by adding another “rung” with two propagator lines at each vertex. The crosses denote field insertions.

and the function $\mathbf{I}(x, y; G)$ sums an infinite series of “rungs” (cf. Fig. 2):

$$\mathbf{I}(x, y; G) = \frac{\lambda}{6N} G_{ab}(x, y) G_{ab}(x, y) - i \frac{\lambda}{6N} \int_z \mathbf{I}(x, z; G) G_{ab}(z, y) G_{ab}(z, y).$$

The 2PI $1/N$ -expansion provides a controlled nonperturbative approximation scheme. It can be in particular applied to critical phenomena near continuous phase transitions, or to nonperturbatively large densities as described below^{13,14}. Instead, for sufficiently dilute systems and weak couplings a 2PI coupling-expansion can be appropriate. The lowest non-trivial order then contains all diagrams with topology as given by the first graph in the upper and lower series presented in Fig. 2.

The systematic expansion schemes discussed above can be straightforwardly applied to fermionic theories as well^{5,11}. As an example, consider a theory with two fermion flavors coupled to an $O(4)$ -vector of scalar fields $\varphi_a \equiv (\sigma, \vec{\pi})$ via a chirally invariant interaction with Yukawa coupling g :

$$V(\varphi; \bar{\psi}, \psi) = \frac{1}{2} m_0^2 (\sigma^2 + \pi^2) - g \bar{\psi} [\sigma + i\gamma_5 \vec{\tau} \cdot \vec{\pi}] \psi. \quad (12)$$

This is a simplified version of the linear sigma model, with no scalar self-interaction, which is sufficient to obtain thermalization as is described below¹¹. The 2PI effective action at lowest nontrivial order in a systematic coupling expansion then contains only the two-loop graph shown in Fig. 3.

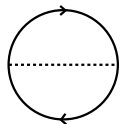


Figure 3. Two loop contribution to Γ_2 . The solid and dashed lines represent the full fermionic (D) and bosonic (G) propagators, respectively.

For discussing nonequilibrium results it is useful to rewrite the propagators in terms of the spectral function ρ and the statistical function F ^{20,9}:

$$G(x, y) = F(x, y) - \frac{i}{2} \rho(x, y) \text{sign}_c(x^0 - y^0) \quad (13)$$

and equivalently for the fermion propagator D . We emphasize that out of equilibrium F and ρ are *independent* functions. However, in thermal equilibrium both functions are related by the fluctuation-dissipation relation, which can be written in Fourier space^{20,9}:

$$F^{(\text{eq})}(\omega, \vec{p}) = -i \left(n_{\text{BE}}(\omega) + \frac{1}{2} \right) \rho^{(\text{eq})}(\omega, \vec{p}), \quad (14)$$

where $n_{\text{BE}}(\omega) = (e^{\omega/T} - 1)^{-1}$ denotes the Bose-Einstein distribution with temperature T . Starting far from equilibrium, Eq. (14) can be used to test thermalization at sufficiently late times¹¹ as is discussed below.

4. Comparison of LO, NLO and exact results

LO vs. NLO: Why is it crucial to go beyond leading-order large- N or Hartree approximations? We consider for a moment the LO contribution, Eq. (8), or the Hartree approximation which also includes the first graph of Fig. 2. This takes into account space-time dependent mass corrections and neglects, in particular, direct scattering. An important consequence is the appearance of an infinite number of conserved quantities, which are not present in the fully interacting or finite- N theory. These can be written as^{9,17}

$$\left[F(t, t'; p) \partial_t \partial_{t'} F(t, t'; p) - (\partial_t F(t, t'; p))^2 \right]_{t=t'}^{1/2} \equiv n_0(p) + \frac{1}{2}, \quad (15)$$

where we have considered a spatially homogeneous situation with $F(t, t'; p)$ denoting the spatial Fourier transform. These additional constants of motion can have a substantial impact on the time evolution, since they strongly constrain the allowed dynamics. As a characteristic example, one may consider the time evolution for so-called “tsunami”²¹ initial conditions with a vanishing field expectation value: A large initial particle number density in a narrow range around a characteristic momentum $p = \pm p_{\text{ts}}$. Here we consider first 1 + 1 dimensions, where the initial condition is reminiscent of two colliding “wave packets” with opposite and equal momentum. The left graph of Fig. 4 shows the *equal-time* two-point function $F(t, t; p)$ as a function of time both for the LO and NLO approximation⁹. One observes that at NLO the highly populated modes around p_{ts} get quickly depopulated, while the density for low momentum modes increases. In contrast,

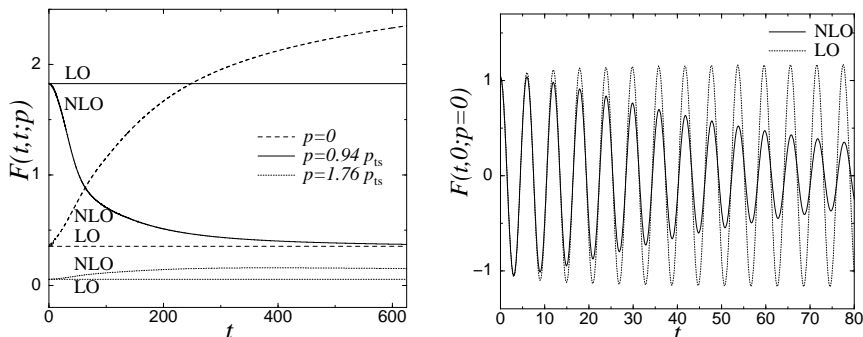


Figure 4. Comparison of results at LO and at NLO in the 2PI $1/N$ -expansion ($N = 10$). **Left:** *Equal-time* two-point function $F(t, t; p)$ for different momenta as a function of time for “tsunami” initial conditions. **Right:** *Unequal-time* two-point function $F(t, 0; p = 0)$ as a function of time following a sudden “quench”. (All in units of the initial-time mass.)

at LO the evolution of the equal-time correlator is trivial. This reflects the fact that at LO or for Hartree approximations, there exists a well-defined particle number for each momentum mode, which does not change in time:⁹ $n_0(p)$ of Eq. (15). This is in sharp contrast to the NLO approximation or the fully interacting real scalar theory, where there is no conserved particle number and the LHS of (15) depends on time. Similarly strong qualitative differences can also be observed for *unequal-time* correlation functions. As an example, we show on the right of Fig. 4 the two-point correlation with the initial time, $F(t, 0; p = 0)$, following a sudden “quench”⁹. After some oscillations one finds that at NLO the unequal-time correlator quickly approaches an exponentially damped behavior. In contrast, at LO no effective suppression is observed. This reflects the fact that at LO the presence of additional constants of motion keep the details about the initial conditions.

NLO vs. exact results: In view of the substantial changes encountered by going from LO to NLO for finite N , one wonders what happens at NNLO or beyond. One can rigorously answer this question in a well-defined limit: Nonequilibrium dynamics in *classical* statistical field theory can be solved *exactly* up to controlled statistical errors, using numerical integration and Monte Carlo techniques^{22,18,23,24,25}. The 2PI $1/N$ -expansion can be equally well implemented in the classical as in the quantum case²⁴. Therefore, in the classical field limit one can compare with results including *all* orders in $1/N$. In particular, for increasing occupation numbers per

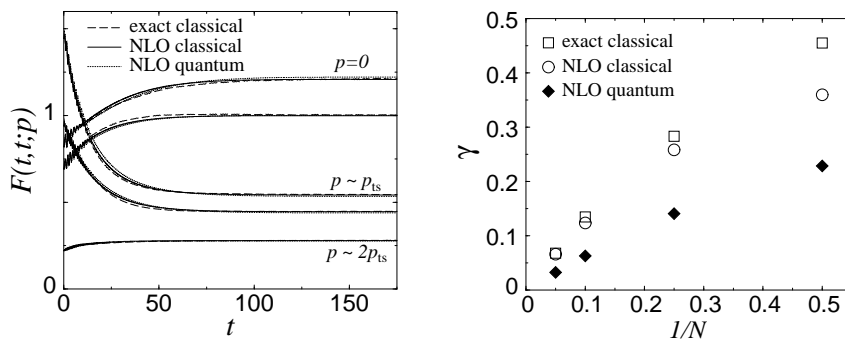


Figure 5. Comparison between exact (MC) results and results from the 2PI $1/N$ -expansion at NLO both for the classical and the quantum field theory. **Left:** Time evolution of the equal-time correlation function for an initial condition similar as for Fig. 4 with high occupation numbers ($N = 4$). **Right:** Damping rate, extracted from the unequal-time correlation function (cf. Fig. 4, right). Here the initial conditions are characterized by low occupation numbers so that quantum effects become sizeable.

mode the classical and the quantum evolution can be shown to approach each other, if the same initial conditions are applied²⁴: For sufficiently high particle number densities one can strictly verify how rapidly the $1/N$ series converges.

Fig. 4 shows a comparison of exact and NLO results²⁴. One observes that the NLO result follows closely the exact solution already for moderate values of N . This concerns both the far-from-equilibrium dynamics at early times as well as the late-time behavior close to equilibrium. The 2PI $1/N$ -expansion exhibits very good accuracy already in lowest nontrivial order! We emphasize that also for low densities, where the classical field approximation provides not a good description for the quantum theory (cf. Fig. 4), a coupling-expansion to three-loop and a $1/N$ -expansion to NLO give very similar results for sufficiently weak coupling and not too small $N \gtrsim 2$. One is lead to conclude that, once the spurious conserved quantities of LO or Hartree approximations are removed by interactions, the results are rather independent of the details of the approximation.

$1/N$ -expansion in the limit $N = 1$: The agreement between NLO and exact results is found to be rather good for values as small as $N \gtrsim 2$ (cf. Fig. 5)²⁴. However, in the limit $N = 1$ subleading contributions in $1/N$ are no longer suppressed and, in particular, the $1/N$ -expansion at NLO exhibits a reduced damping rate^b. The case $N = 1$ has been investigated in classical field theory in Ref. 25 for initial conditions with zero and nonzero field ϕ . An approximation, which includes part of the NNLO corrections, such as BVA¹⁵, is found to give a better damping rate for the field. However, a worse result is obtained for the two-point function, which reflects the absence of an expansion parameter for $N = 1$. For weak interactions a systematic expansion can be based on the 2PI coupling-expansion for $N = 1$.

Spontaneous symmetry breaking: It is a well-known fact that there is no spontaneous symmetry breaking in one spatial dimension at nonzero temperature or energy density. In contrast, LO or Hartree approximations can exhibit a phase transition independent of the number of dimensions. For nonequilibrium, Cooper et al. have pointed out in Ref. 10 that the 2PI $1/N$ -expansion at NLO shows no spontaneous symmetry breaking in one spatial

^bWe note that this can be understood from the fact that the three-loop contribution to the 2PI effective action (which gives the lowest order contribution to the damping rate in a coupling expansion) is $\sim (\lambda/N)^2[1 + 2/N]$. Comparing this with the corresponding three-loop contribution at NLO in the $1/N$ -expansion^{9,12} for $N = 1$, one finds a factor of three less for the latter (cf. Sect. 3).

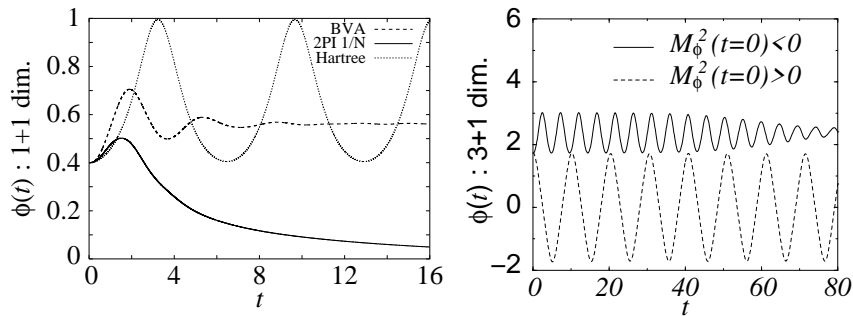


Figure 6. Examples of nonequilibrium time evolutions of the field expectation value $\phi(t)$ for one (left¹⁰) and for three (right) spatial dimensions using different approximations. The 2PI $1/N$ -expansion (here for the limit $N = 1$) correctly describes the absence of a spontaneously broken phase in one spatial dimension, with $\phi(t) \rightarrow 0$ at late times. In contrast, spontaneous symmetry breaking can be observed at NLO in $3 + 1$ dimensions.

dimension, thus curing the problem of mean-field type approximations. As an example, the left graph of Fig. 6 (taken from Ref. 10) shows their results for the time evolution of the field expectation value $\phi(t)$. One observes that, while the Hartree approximation oscillates around a nonzero field value, the NLO result tends to the symmetric phase with $\phi = 0$. We emphasize, however, that the latter results have been obtained from a $1/N$ -expansion in the uncontrolled limit $N = 1$. This becomes obvious once e.g. a part but not all of the NNLO contributions are taken into account, as denoted by BVA in Fig. 6, where again one finds spontaneous symmetry breaking in one spatial dimension. More recent results, demonstrating the absence of a nonequilibrium phase transition in one spatial dimension have been obtained from a loop-expansion in a related (2PPI) approximation scheme¹⁶. It is interesting that the systematic $1/N$ -expansion is found to give qualitatively correct results even for $N = 1$. Here we show for the first time that the 2PI $1/N$ -expansion exhibits spontaneous symmetry breaking in $3 + 1$ dimensions. The right graph of Fig. 6 shows the evolution for a sufficiently negative and a positive initial mass parameter M_ϕ^2 , which leads to a nonzero and a vanishing field expectation value respectively.

5. Applications

5.1. Parametric resonance in quantum field theory

In classical mechanics parametric resonance is the phenomenon of resonant amplification of the amplitude of an oscillator having a time-dependent periodic frequency. In the context of quantum field theory a similar phe-

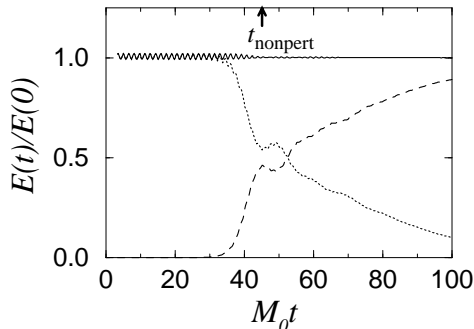


Figure 7. Total energy (solid line) and classical field energy (dotted line) as a function of time for $\lambda = 10^{-6}$. The dashed line represents the fluctuation part, showing a transition between a classical field and a fluctuation dominated regime.

phenomenon describes the amplification of quantum fluctuations, which can be interpreted as particle production. It provides an important building block for our understanding of the (pre)heating of the early universe at the end of an inflationary period²⁶, and may also be operative in various situations in the context of relativistic heavy-ion collisions²⁷.

The phenomenon of parametric resonance provides a paradigm for the dynamics of quantum fields at nonperturbatively large densities^c. It is a far-from-equilibrium phenomenon involving the production of particles with densities inversely proportional to the coupling. For this reason, it has been much studied in the classical field approximation, which has long been the only available quantitative approach²⁹. Studies in quantum field theory have so far been limited to linear or mean-field type approximations²⁶.

Using the methods described in the previous sections, recently the first quantum field theoretical study of this phenomenon beyond LO or Hartree approximations has been performed¹³. To deal with the nonperturbatively large densities, one can employ the 2PI $1/N$ -expansion at NLO, in the presence of a nonvanishing field (the “inflaton”) in $3 + 1$ dimensions.

We consider¹³ a system that is initially in a pure quantum state, characterized by a large field amplitude $\phi_a(t = 0) \sim 1/\sqrt{\lambda}$ and comparatively small quantum fluctuations, described here by employing vanishing particle numbers at initial time. Fig. 7 provides an overview of the dynamics: At early times, the total energy of the system is dominated by the contribution from the large field amplitude, which subsequently decays into

^cAnother important example, where nonperturbatively high densities occur, is provided by the physics of the color glass condensate²⁸ in QCD.

particles, giving rise to a fluctuation dominated regime at late times. More precisely, the early time coherent oscillations of the field trigger an exponential amplification of quantum fluctuations, corresponding to explosive particle production in a narrow range of momenta centered at $p = p_0$: this is parametric resonance.²⁶ Later on, nonlinear interactions between field modes cause this amplification to propagate to higher momenta. More specifically, the initially amplified modes act as a source for other modes. This source-induced amplification results in an enhanced particle production in a broad momentum range. This is illustrated in Fig. 8, where the effective particle number is shown for various momenta as a function of time from a numerical solution.

We emphasize that, using the above 2PI techniques, one can obtain the main features of the nonlinear dynamics up to t_{nonpert} also from an analytical solution of the evolution equations¹³. In particular, in order for the NLO effects to be small compared to LO dynamics at early times, one needs values of N as large as $N \gtrsim 1/\lambda$. The late-time dynamics for $t \gg t_{\text{nonpert}}$ requires the numerical solution of the NLO equations. For the employed small couplings, this involves extremely large times which has not been undertaken up to now. It has recently been shown using classical field theory methods that the very slow subsequent evolution is characterized by turbulent behavior³⁰. However, to describe the late-time approach to quantum thermal equilibrium with a Bose-Einstein distributed particle number, one needs to go beyond the classical field approximation.

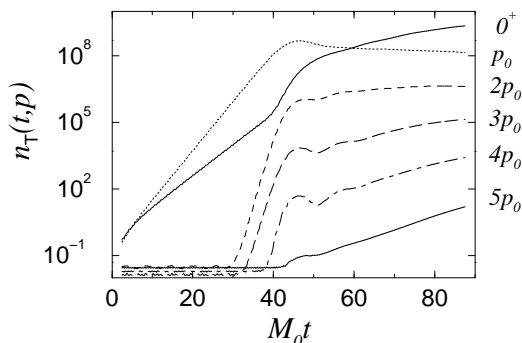


Figure 8. Effective particle number density for the transverse modes as a function of time for various momenta $0 \leq p \leq 5p_0$ and $\lambda = 10^{-6}$. At early times, modes with momentum $p \simeq p_0$ are exponentially amplified with a rate $\sim 2\gamma_0$ via the mechanism of parametric resonance. Due to nonlinearities, one observes subsequently an enhanced growth with rate $\sim 6\gamma_0$ for a broad momentum range.

5.2. Nonequilibrium chiral quark-meson model

We consider a theory involving two Dirac fermion flavors (“quarks”) coupled to a scalar σ -field and a triplet of pseudoscalar “pions” as described by Eqs. (6). Such type of linear σ -models, which implement the approximate chiral $SU_L(2) \times SU_R(2)$ symmetry of QCD, can be a useful first guide for the behavior of strongly interacting matter relevant for the dynamics of relativistic heavy-ion collisions.

Recently¹¹ the far-from-equilibrium time evolution and subsequent thermalization has been described for this model at lowest nontrivial order in the 2PI coupling-expansion, corresponding to the two-loop graph presented in Fig. 3. Starting from various different far-from-equilibrium initial conditions, one finds a universal late-time behavior that is only determined by the expectation value of the initial energy density. In particular, one is able to observe the approach to Bose-Einstein and Fermi-Dirac distributions at sufficiently late times. Similar studies of the late-time behavior have previously only been performed for purely scalar theories in $1+1$ dimensions^{8,9}.

As an example, in Figs. 9 and 10 the statistical two-point functions for the fermions, $F_V(t, t; p)$, and for the scalars, $F_\phi(t, t; p)$, are shown for two very different nonequilibrium initial conditions (cf. Ref. 11 for details). One observes that the time evolution becomes soon rather insensitive to the details of the initial condition. The time for the effective loss of initial conditions is well described by the inverse damping rate obtained from the respective unequal-time two-point function (cf. the example in Fig. 4). In

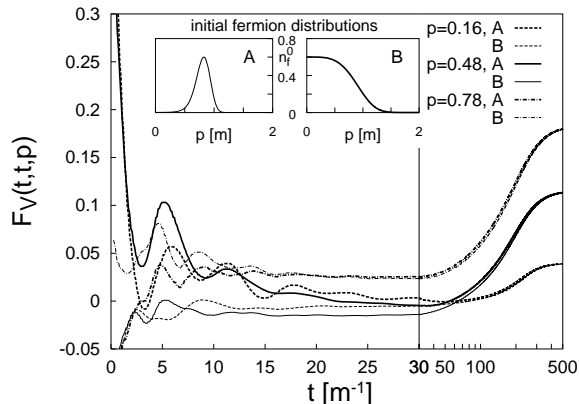


Figure 9. Time evolution of fermionic equal-time two-point functions for various momenta and for two different initial conditions A and B . The corresponding initial particle number distributions, shown in the insets, are chosen such that the total energy is the same for both cases. (In units of the scalar *thermal* mass m .)

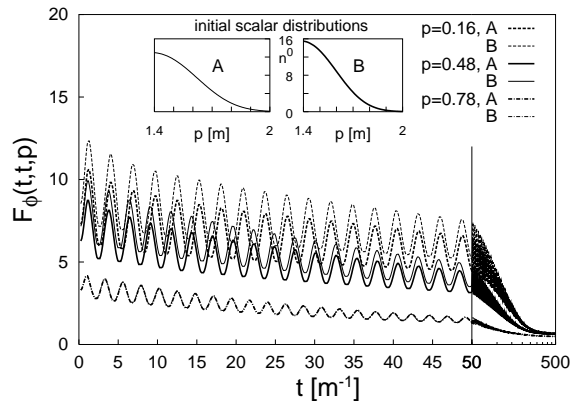


Figure 10. Same as in Fig. 9 but for the scalars.

contrast, this time scale does not characterize the late-time behavior. For the latter, one finds, to very good approximation, an exponential relaxation of each mode to their universal late-time values. For the employed initial conditions the thermalization rate is somewhat larger than the damping rate. Though quantitatively very different, a similar qualitative behavior has been previously observed for scalar theories in $1 + 1$ dimensions^{8,9}.

At sufficiently late times one can explicitly demonstrate the approach to quantum thermal equilibrium^d: Out of equilibrium, the spectral and statistical two-point functions are completely independent in general. However, if thermal equilibrium is approached, they have to become related by the fluctuation-dissipation relation at late times as stated in Eq. (14). For sufficiently late times one observes that the correlators become approximately homogeneous in time and a Fourier transform with respect to $t - t'$ can be performed to very good approximation. The result is shown in Fig. 11.

This work provides an important first step for a quantitative description of realistic theories with fermions in $3 + 1$ dimensions, with important phenomenological applications³¹ to the out-of-equilibrium chiral phase transition, or the physics of baryogenesis in the early universe³².

^dWe emphasize that thermal equilibrium cannot be reached on a fundamental level from time-reversal invariant evolution equations at any finite time. The results demonstrate^{8,9,11} that thermal equilibrium can be approached very closely at sufficiently late time, without again deviating from it for practically accessible times.

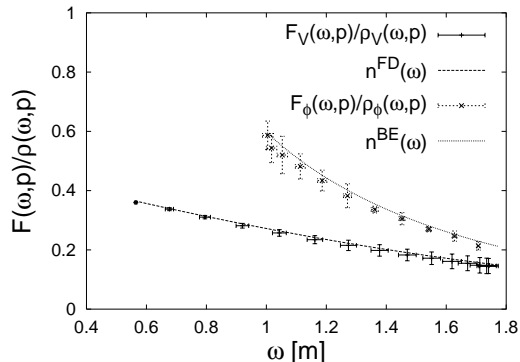


Figure 11. The late-time ratio of the statistical two-point function and the spectral function in frequency space, both for fermions (F_V/ρ_V) and for scalars (F_ϕ/ρ_ϕ). For thermal equilibrium the quotient has to correspond to the Bose-Einstein (BE) distribution for scalars and to the Fermi-Dirac (FD) distribution for fermions. The BE/FD distributions are displayed by the continuous curves with the same temperature $T = 0.94m$.

6. Outlook

The 2PI generating functional for Green’s functions provides a powerful technique for nonequilibrium physics. Systematic approximation schemes can describe far-from-equilibrium dynamics as well as subsequent thermalization from “first principles”. Substantial progress has been achieved along these lines in recent years and, by now, the methods provide a practical means for quantitative descriptions of realistic scalar and fermionic quantum field theories. Apart from the discussed applications motivated by high-energy particle physics and cosmology, we emphasize that the same techniques can be applied to condensed matter systems. As an important example, the dynamics of Bose-Einstein condensation can be addressed along very similar lines.

One important issue, which we have not discussed here, concerns the renormalizability of approximations based on truncations of the 2PI effective action. To prove this is a nontrivial task because of the fully self-consistent character of these approximations. Recent work has shown that, in the context of scalar field theory, approximations based on a systematic loop-expansion of the 2PI effective action (“ Φ -derivable approximations”) can be renormalized order by order, if the underlying theory is perturbatively renormalizable^{33,34,35}.

Another, major open question concerns the description of gauge fields. The difficulty is related to the fact that truncations of the 2PI effective

action in general violate Ward identities. One possibility to avoid this difficulty is to modify the 2PI-based approximations in such a way as to enforce Ward identities. Practical examples in this direction have been pointed out for nonequilibrium systems³⁶. Another interesting possibility is to try to keep the gauge dependence of physical results under control. This has recently been investigated in Ref. 37 and further interesting developments are to be awaited.

Acknowledgments

We thank Gert Aarts, Daria Ahrensmeier, Rudolf Baier, Szabolcs Borsányi, Jürgen Cox, Markus M. Müller and Christof Wetterich for very fruitful collaborations on this topic.

References

1. See e.g. D. Bödeker, Nucl. Phys. Proc. Suppl. **94** (2001) 61; J. P. Blaizot, E. Iancu, Phys. Rept. **359** (2002) 355; L. G. Yaffe, hep-ph/0010249.
2. See also the contributions of L. Yaffe, of G. Moore and of T. Prokopec, these proceedings.
3. P. Braun-Munzinger, J. Stachel, J. Phys. **G28** (2002) 1971; U. W. Heinz, P. F. Kolb, Proceedings of the 18th Winter Workshop on Nuclear Dynamics. Edited by R. Bellwied, J. Harris, W. Bauer. EP Systema, Debrecen, Hungary, 2002. pp. 205-216 [hep-ph/0204061].
4. J. Serreau, D. Schiff, JHEP **0111** (2001) 039; R. Baier, A.H. Mueller, D. Schiff, D. T. Son, Phys. Lett. **B502** (2001) 51; Phys. Lett. **B539** (2002) 46.
5. J. M. Luttinger, J. C. Ward, Phys. Rev. **118** (1960) 1417; G. Baym, Phys. Rev. **127** (1962) 1391; J. M. Cornwall, R. Jackiw, E. Tomboulis, Phys. Rev. **D10** (1974) 2428.
6. L.P. Kadanoff, G. Baym, *Quantum Statistical Mechanics*, Benjamin, New York (1962); P. Danielewicz, Annals Phys. **152** (1984) 239; P. Lipavský, V. Spicka, K. Morawetz, Annales de Physique **26** (2001) 1;
7. K. C. Chou, Z. B. Su, B. L. Hao, L. Yu, Phys. Rept. **118** (1985) 1; E. Calzetta, B. L. Hu, Phys. Rev. **D37** (1988) 2878; Y. B. Ivanov, J. Knoll, D. N. Voskresensky, Nucl. Phys. **A657** (1999) 413.
8. J. Berges, J. Cox, Phys. Lett. **B517** (2001) 369.
9. J. Berges, Nucl. Phys. **A699** (2002) 847.
10. F. Cooper, J. F. Dawson, B. Mihaila, hep-ph/0209051.
11. J. Berges, S. Borsányi, J. Serreau, to be published in Nucl. Phys. B [hep-ph/0212404].
12. G. Aarts, D. Ahrensmeier, R. Baier, J. Berges, J. Serreau, Phys. Rev. **D66** (2002) 045008.
13. J. Berges, J. Serreau, hep-ph/0208070.
14. J. Berges, M. M. Müller, Proceedings of the 285th Heraeus Seminar: Interdisciplinary Workshop on *Progress in Nonequilibrium Greens Functions*, Dresden, Germany, 2002 [hep-ph/0209026].

15. B. Mihaila, F. Cooper, J. F. Dawson, Phys. Rev. **D63** (2001) 096003;
16. J. Baacke, A. Heinen, hep-ph/0212312.
17. Among the extensive literature on Gaussian approximations see e.g. D. Boyanovsky, H. J. de Vega, Phys. Rev. **D47** (1993) 2343; F. Cooper, S. Habib, Y. Kluger, E. Mottola, J. P. Paz, P. R. Anderson, Phys. Rev. **D50** (1994) 2848; D. Boyanovsky, H. J. de Vega, R. Holman, D. S. Lee, A. Singh, Phys. Rev. **D51** (1995) 4419; F. Cooper, S. Habib, Y. Kluger, E. Mottola, Phys. Rev. **D55** (1997) 6471; J. Baacke, K. Heitmann, C. Pätzold, Phys. Rev. **D58** (1998) 125013 .
18. G. Aarts, J. Smit, Phys. Rev. **D61** (2000) 025002; L. M. Bettencourt, K. Pao, J. G. Sanderson, Phys. Rev. **D65** (2002) 025015; M. Sallé, J. Smit, J. C. Vink, Nucl. Phys. **B625** (2002) 495; M. Sallé, J. Smit, hep-ph/0208139;
19. L. M. Bettencourt, C. Wetterich, Phys. Lett. **B430** (1998) 140; B. Mihaila, T. Athan, F. Cooper, J. Dawson, S. Habib, Phys. Rev. **D62** (2000) 125015; A. V. Ryzhov, L. G. Yaffe, Phys. Rev. **D62** (2000) 125003.
20. G. Aarts, J. Berges, Phys. Rev. **D64** (2001) 105010.
21. D. Boyanovsky, H. J. de Vega, R. Holman, S. Prem Kumar, R. D. Pisarski, Phys. Rev. **D57** (1998) 3653.
22. G. Aarts, G. F. Bonini, C. Wetterich, Phys. Rev. **D63** (2001) 025012.
23. Sz. Borsányi, Zs. Szép, Phys. Lett. **B508** (2001) 109.
24. G. Aarts, J. Berges, Phys. Rev. Lett. **88** (2002) 041603; J. Berges, Nucl. Phys. **A702** (2002) 351.
25. K. Blagoev, F. Cooper, J. Dawson, B. Mihaila, Phys. Rev. **D64** (2001) 125003; F. Cooper, J. F. Dawson, B. Mihaila, hep-ph/0207346.
26. L. Kofman, A. D. Linde, A. A. Starobinsky, Phys. Rev. Lett. **73** (1994) 3195; D. Boyanovsky, H. J. de Vega, R. Holman, J. F. Salgado, Phys. Rev. **D54** (1996) 7570.
27. See e.g. A. Dumitru, R. D. Pisarski, Phys. Lett. **B504** (2001) 282; S. Mrówczyński, B. Müller, Phys. Lett. **B363** (1995) 1; D. Ahrensmeier, R. Baier, M. Dirks, Phys. Lett. **B484** (2000) 58.
28. See the different contributions to these proceedings by E. Iancu, R. Baier, J.-P. Blaizot and L. McLerran.
29. S. Y. Khlebnikov, I. I. Tkachev, Phys. Rev. Lett. **77** (1996) 219; T. Prokopec, T. G. Roos, Phys. Rev. **D55** (1997) 3768.
30. I. I. Tkachev, these proceedings; R. Micha, I. I. Tkachev, hep-ph/0210202.
31. J. Serreau, contribution to the “CERN Yellow Report on Hard Probes in Heavy Ion Collisions at the LHC” (2003).
32. T. Prokopec, these proceedings; see also K. Kainulainen, T. Prokopec, M. G. Schmidt, S. Weinstock, COSMO-01, hep-ph/0201245.
33. H. van Hees, J. Knoll, Phys. Rev. **D65**, 025010 (2002); 105005 (2002).
34. U. Reinosa, these proceedings; J.-P. Blaizot, E. Iancu, U. Reinosa, hep-ph/0301201
35. Cf. also E. Braaten, E. Petitgirard, Phys. Rev. **D65** (2002) 085039.
36. E. Mottola, these proceedings; see also SEWM 2001, Marseille, France.
37. A. Arrizabalaga, these proceedings; A. Arrizabalaga, J. Smit, Phys. Rev. **D66** (2002) 065014.